Research Article Vol. 59, No. 5 / 10 February 2020 / Applied Optics A135

applied optics

# Effect of an optical coating on in-band and out-of-band transmitted and reflected wavefront error measurements

Graham Carlow,* Brian T. Sullivan, Claude Montcalm, and Alexander Miles

*Iridian Spectral Technologies Ltd., 2700 Swansea Crescent, Ottawa, Ontario K1G 6R8, Canada*
**Corresponding author: graham.carlow@iridian.ca*

*Received 17 September 2019; revised 8 November 2019; accepted 28 November 2019; posted 2 December 2019 (Doc. ID 378163); published 10 January 2020*

**The wavefront error (WE) of a surface with an optical coating ("filter") is ideally measured at the in-band wavelength of the filter. However, quite often this is not possible, requiring that the filter be measured at an out-of-band wavelength (typically 633 nm), assuming that the filter transmits (for transmitted WE, or TWE) or reflects (for reflected WE, or RWE) at this wavelength. This out-of-band TWE/RWE is generally assumed to provide a good estimation of the desired in-band TWE/RWE. It will be shown in this paper that this is not the case for a large class of filters (i.e., bandpass) where the group delay is significantly different at the in-band and out-of-band wavelengths and where the optical filter exhibits a thickness non-uniformity across the surface. A theoretical explanation will be given along with an approach to predict the in-band TWE/RWE based on the coating non-uniformity, the measured out-of-band TWE/RWE, and the theoretical properties of the optical filter at the in-band and out-of-band wavelengths. A reasonable agreement between theory and measurement was demonstrated by measuring the TWE of an 11 nm wide bandpass filter (centered at 1048 nm) at both in-band ($\lambda = 1048$ nm) and out-of-band ($\lambda = 625$ nm) wavelengths. A similar treatment is provided for RWE.** © 2020 Optical Society of America

https://doi.org/10.1364/AO.59.00A135

## 1. INTRODUCTION

For a number of imaging applications involving optical coatings or filters, the transmitted wavefront error (TWE) and/or the reflected wavefront error (RWE) is an important filter specification [1]. The TWE (RWE) is usually specified as a fraction of a wave at a specific wavelength over a specified spatial distance or in units of nanometers specifying the allowed *peak-to-valley* [pv] variation or the root-mean-square [*rms*] variation. If the filter's measured TWE[pv] (or RWE[pv]) value exceeds the allowed specification, this can result in imaging problems; however, it should be noted that spherical and tilt contributions can usually be subtracted out of the filter's TWE value if the optical system in which the filter is used can compensate for these aberrations [1]. In this and the next section, the difference in TWE for the "in-band" and "out-of-band" wavelengths will be first investigated. A similar approach is then used for RWE.

The TWE of an optical filter is affected in different ways by an optical coating, and this has been previously investigated by a number of authors [2–9]. First, the optical coating stress can cause a substrate curvature; however, this will only have a small effect on the TWE. Second, there is a phase change in the light as it passes through the coating. If the coating thickness is uniform across the filter's clear aperture, then the phase change does not result in a wavefront distortion (WFD); however, if there is a coating thickness non-uniformity, then a WFD can occur that will affect the TWE. The importance of taking into account the TWE/RWE caused by optical coatings for different filter applications has been recently investigated by several groups [9–13].

Typically, the TWE of an optical filter is measured on a commercial interferometer operating a wavelength of 633 nm. In most cases, this is an out-of-band wavelength for the optical filter. The motivation for this paper is to highlight the fact that an out-of-band TWE measurement can be substantially different (i.e., lower) compared to the actual in-band TWE of the optical filter, depending on the uniformity of the optical coating and the filter design. It will also be shown that the actual in-band TWE value can be estimated from (i) the measured out-of-band TWE value and (ii) the difference in the WFD between the in-band and out-of-band wavelengths.

In the next section, a review of how an optical coating can result in a WFD is presented. To provide physical insight into the causes of the WFD, a first-order equation is derived as well. Then, to demonstrate the substantial variation between the in-band and out-of-band TWE values, a bandpass filter centered at $\lambda = 1048$ nm with a full width half-maximum (FWHM) of

11 nm was designed and fabricated. The TWE of this filter was measured using a multiwavelength wavefront sensor [14] with a LED light source centered at $\lambda' = 625$ nm (for the out-of-band wavelength) and with a 1040–1060 nm tunable laser (for the in-band wavelengths). The measured in-band TWE results are compared to the theoretically predicted in-band TWE values. After this, a similar systematic investigation of the RWE for an optical filter is also carried out.

## 2. WAVEFRONT DISTORTION

The WFD arising from the non-uniformity of an optical coating can be explained with the help of Fig. 1, which shows a schematic of a light ray incident upon a non-uniform optical coating. The phase convention and notations are defined in the figure caption. Note that the substrate curvature arising from coating stress is neglected in this diagram.

Using the notation of [4], the phase variation at a radius $r$, $\varphi_{\mathrm{WF}}$, is the sum of the phase variation in the entrance medium and in the coating, $\varphi_o$ and $\varphi_T$, respectively. If the coating thickness is $d$ at a radius $r$, then because $s(r) + d(r) = L$, the phase variation resulting in a WFD can be written as

$$\varphi_{\mathrm{WF}}(\lambda, d) = \varphi_T(\lambda, d) + \varphi_o(\lambda, L - d),$$
$$\text{where } \varphi_o(\lambda, z) = \frac{-2\pi \cdot n_o z \cdot \cos(\theta_o)}{\lambda}, \tag{1}$$

where $\varphi_T(\lambda, d)$ can be calculated from the filter design (i.e., using a thin film program), and $\theta_o$ is the angle of incidence. As pointed out in [4], it is important to include the entrance medium phase contribution. The WFD is then given by $-\lambda \cdot \varphi_{\mathrm{WF}}(\lambda, d)/2\pi$ (in nanometers), where the minus sign is required to convert from the thin film phase convention to the optics phase convention. The next step is to calculate the difference in the WFD resulting from a coating non-uniformity, i.e., between a thickness "$d + \delta d$" and "$d$":

$$\Delta\mathrm{WFD} = \frac{-\lambda}{2\pi}\{\varphi_{\mathrm{WF}}(\lambda, d + \delta d) - \varphi_{\mathrm{WF}}(\lambda, d)\},$$
$$\text{in units of the wavelength, i.e., nm,} \tag{2}$$

or, using Eq. (1):

$$\Delta\mathrm{WFD} = \frac{-\lambda}{2\pi}\{[\varphi_T(\lambda, d + \delta d) - \varphi_T(\lambda, d)] + \varphi_o(\lambda, -\delta d)\}. \tag{3}$$

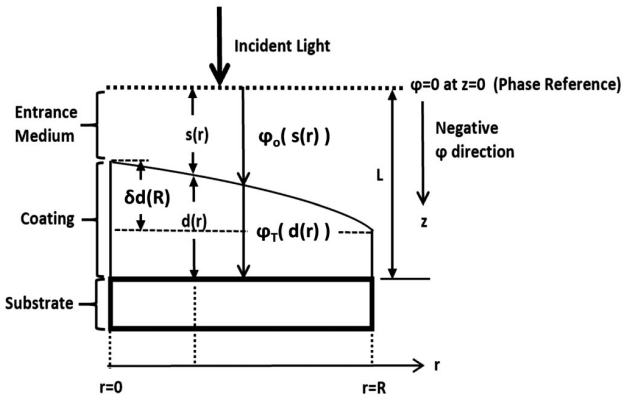


**Fig. 1.** Schematic of light incident upon a non-uniform optical coating (may consist of multiple layers). An arbitrary phase reference line is placed a distance $L$ from the substrate. With the thin film phase convention, $\exp -\{ikz\}$, where $k$ is the wavenumber, the phase becomes more negative along the positive $z$ direction. In this schematic, the angle of incidence $\theta_o$ is 0° and the entrance medium has a refractive index $n_o$. The phase change across the entrance medium starting from the phase reference line is represented by $\varphi_o$ whereas $\varphi_T$ is phase change from the coating interface to the substrate interface. At any radius, $r$, the distance in the entrance medium from the phase reference line to the coating interface is $s(r)$, whereas the coating thickness is $d(r)$. The difference in thickness at any radius $r$ is given by $\delta d(r) = d(r = 0) - d(r)$, thus ensuring that sign of $\delta d(r)$ is consistent with the $z$-axis direction.

$\Delta$WFD is the portion of the TWE resulting from the optical coating non-uniformity, and this can be calculated exactly using a thin film program. For an optical coating consisting of low- and high-index materials, the $\delta d$ change can consist of $\delta d_L$ and $\delta d_H$ values based on different uniformities for the low- and high-index materials, respectively. Note that some authors calculate $\Delta$WFD using the change in phase based on the wavelength shift associated with the thickness variation; however, this is not accurate if there is a significant optical constant dispersion in the coating materials.

Although Eq. (3) is exact, it is useful to have additional insight into the properties of the optical coating that result in the WFD. Assuming that the low- and high-index uniformities are the same, then if all of the layers in the optical coating are scaled by $\beta = 1 + \alpha$, then $\alpha \equiv -\delta d/d$ is a measure of the thickness non-uniformity. (The minus sign in $\alpha$ is required because the uniformity is defined with the delta thickness usually measured with respect to the substrate plane—opposite to the direction of how $\delta d$ is defined in Fig. 1). One can then show, to first order in a Taylor expansion of the phase (see Appendix A), that:

$$\Delta\mathrm{WFD} \approx \alpha(r) \cdot \{\eta(\lambda) \cdot \mathrm{GD}(\lambda) \cdot c - n_o \cdot d\cos(\theta_o)\}, \tag{4}$$

where group delay $(\mathrm{GD})(\lambda)(= -d\varphi_T/d\omega)$ is the transmittance GD [ps] of the filter at a wavelength $\lambda$, $\omega$ is the angular frequency, $c$ is the speed of light [nm/ps], and $\eta(\lambda) \equiv |(\lambda/\delta\lambda)/(d/\delta d)|$ is a term that takes into account the material optical dispersion in the coating design. Typically, $\eta \sim 0.9 - 1.0$, and it is exactly equal to 1 if there is no optical dispersion in the low- and high-index materials of the optical coating. For a single layer of index $n$ and metric thickness $d$, it can be readily shown that $\eta(\lambda) \approx 1/(1 - \frac{\partial n}{\partial \lambda} \cdot d)$.

From the simplified Eq. (4), it is clear that the change in WFD because of a coating non-uniformity scales with the GD of the filter at the wavelength of interest. If the GD is large, then one can expect a large change in the WFD if there is a significant coating non-uniformity. For filters with a high GD and that have a tight TWE specification, it is critical to minimize the thickness non-uniformity. Note that the GD of an optical coating can be readily calculated from the numerical derivative of the (continuous) transmittance phase as a function of angular frequency.

## 3. IN-BAND TWE

As mentioned previously, sometimes the TWE of a filter can only be measured at an out-of-band wavelength ($\lambda'$). It would be useful to estimate, based on this TWE measurement, the in-band TWE at a wavelength ($\lambda_o$). Let

$$\mathrm{TWE}(\lambda, r) = \widetilde{\mathrm{TWE}}(\lambda, r) + \Delta\mathrm{WFD}(\lambda, r), \tag{5}$$

where $\widetilde{\mathrm{TWE}}(\lambda, r)$ is the component of the TWE that is not related to the coating non-uniformity (i.e., includes wavelength-independent factors, such as intrinsic substrate curvature, inhomogeneities or polishing imperfections, and coating stress-induced curvature). Then, if one ignores the dispersion in the entrance medium between $\lambda'$ and $\lambda_o$, it can be shown,

$$\mathrm{TWE}(\lambda_o, r) = \mathrm{TWE}(\lambda', r) + \{\Delta\mathrm{WFD}(\lambda_o, r) - \Delta\mathrm{WFD}(\lambda', r)\}. \tag{6}$$

Note that the entrance medium phase correction in $\Delta$WFD will cancel out. Then, to first order using Eq. (4),

$$\mathrm{TWE}(\lambda_o, r) = \mathrm{TWE}(\lambda', r) + \alpha(r) \cdot c\{\eta(\lambda_o) \cdot \mathrm{GD}(\lambda_o) - \eta(\lambda') \cdot \mathrm{GD}(\lambda')\}. \tag{7}$$

Equation (6) provides a method of estimating the in-band $\mathrm{TWE}(\lambda_o, r)$ using (i) the measured out-of-band $\mathrm{TWE}(\lambda', r)$, (ii) the change in the GD of the filter between the wavelengths $\lambda_o$ and $\lambda'$, and (iii) the thickness variation. If both the in-band and out-of-band TWE values can be measured, then $\Delta\mathrm{TWE}(\lambda_o, \lambda', r) \equiv \mathrm{TWE}(\lambda_o, r) - \mathrm{TWE}(\lambda', r)$ can be calculated and, using Eq. (7), related to the coating non-uniformity as follows:

$$\Delta\mathrm{TWE}(\lambda_o, \lambda', r) = \alpha(r) \cdot \frac{\partial\Delta\mathrm{TWE}(\lambda_o, \lambda')}{\partial\alpha}, \tag{8}$$

where

$$\frac{\partial\Delta\mathrm{TWE}(\lambda_o, \lambda')}{\partial\alpha} = c\{\eta(\lambda_o) \cdot \mathrm{GD}(\lambda_o) - \eta(\lambda') \cdot \mathrm{GD}(\lambda')\} \approx [\mathrm{GD}(\lambda_o) - \mathrm{GD}(\lambda')] \cdot c. \tag{9}$$

The final approximation holds if it is assumed that $\eta(\lambda') \approx \eta(\lambda_o) \approx 1$. Equation (9) provides a simple rule of thumb to see if a difference in TWE between two different wavelengths is significant based on the GD of the filter at those wavelengths. As well, Eq. (8) can be used to determine the slope, $\partial\Delta\mathrm{TWE}(\lambda_o, \lambda')/\partial\alpha$, from measured data and compare it to the theoretical prediction given by Eq. (9).

Similar arguments can be applied when investigating the RWE. In this case, there is double the contribution from the entrance phase medium because the light transverses this region twice. The equivalent to Eqs. (3) and (4) for the reflectance wavefront distortion (RWFD) is

$$\Delta\mathrm{RWFD} = \frac{-\lambda}{2\pi}\{[\varphi_R(\lambda, d + \delta d) - \varphi_R(\lambda, d)] + \varphi_o(\lambda, -2 \cdot \delta d)\}, \tag{10}$$

$$\Delta\mathrm{RWFD} \approx \alpha(r) \cdot \{\eta(\lambda) \cdot \mathrm{GDR}(\lambda) \cdot c - 2 \cdot n_o \cdot d\cos(\theta_o)\}. \tag{11}$$

With the above two equations, the contribution of the coating non-uniformity on the RWE can be calculated in a similar way as that outlined for Eqs. (5)–(9) with RWE and $\Delta$RWFD substituting for TWE and $\Delta$WFD, respectively, and using the reflectance group delay (GDR) instead of the transmittance GD.

## 4. 1048 nm BANDPASS FILTER: DESIGN, DEPOSITION, AND OPTICAL MEASUREMENTS

To verify the above expressions, a four-cavity bandpass filter, centered at $\lambda_o = 1048$ nm with a FWHM of 11 nm, was designed using low- and high-index materials, $SiO_2$ and $Ta_2O_5$, respectively. With this design, there are a series of transmittance peaks around $\lambda' = 625$ nm so that this out-of-band wavelength can be used for TWE measurements. This filter was then deposited using a reactive magnetron sputtering process on a 125 mm diameter, 6 mm thick fused silica substrate. After deposition, the transmittance of the 1048 nm filter was measured at normal incidence ($\theta_o = 0°$) at wavelengths from 600 to 1100 nm across the substrate.

To measure the TWE of this filter, a multiwavelength wavefront sensor measurement system was used [14]. This instrument has a silicon-based CCD detector allowing the TWE to be measured at any wavelength in the 600–1100 nm wavelength region. For the $\lambda' = 625$ nm spectral region, a LED light source was employed, and for the 1040–1060 nm spectral region, a tunable laser was used. After coating, the TWE of the coated substrate was measured at wavelengths of 625 and 1048 nm along with additional TWE measurements taken every 1 nm over the bandpass wavelength range from 1045 to 1053 nm to study how the TWE varies across the filter bandpass region.

Figure 2 shows the measured TWE of the 1048 nm bandpass filter at wavelengths of 625 and 1048 nm; the TWE[pv] values were 50 and 166 nm, respectively. Based on these measurements, it is clear that there is a significant difference in the WFD between the in-band and out-of-band wavelengths. Notice that because of the different TWE profiles at these two wavelengths, that the WFD is larger than what might be expected based on the TWE[pv] values alone.

The coating non-uniformity, $\Delta d/d$, shown in Fig. 3(a), was determined by dividing the measured $\Delta\lambda/\lambda$ variation by $\eta(\lambda_o = 1048\ \mathrm{nm})$. The wavelength variation $\Delta\lambda/\lambda$ (to within 0.01% accuracy) comes from the measured transmittance of the coating by determining the peak wavelength around $\lambda_o = 1048$ nm. The scatter in the vertical axis is because of azimuthal variation for a given radius. The total metric thickness variation of the filter was $\sim$ 0.19% over the clear aperture ($r = 40$ mm).

## 5. TWE ANALYSIS

To see how well the in-band TWE can be explained by theory, it is first necessary to calculate the filter phase and GD (to check

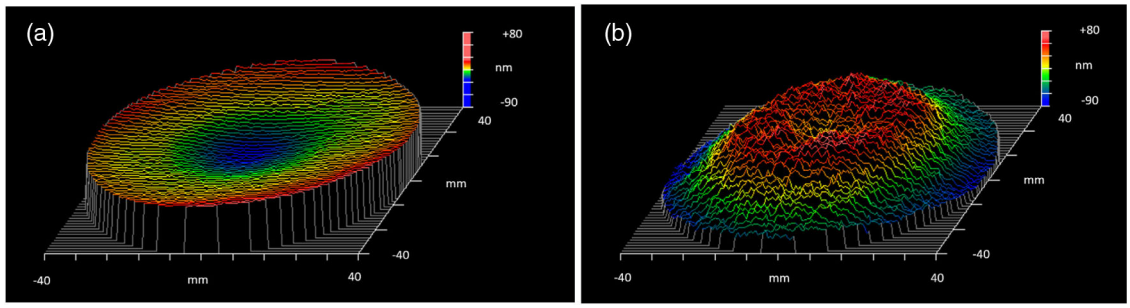


**Fig. 2.** Measured TWE (in nanometers) of the 1048 nm filter at (a) $\lambda' = 625$ nm and (b) $\lambda_o = 1048$ nm. Note the significant difference in wavefront profiles between the two wavelengths.

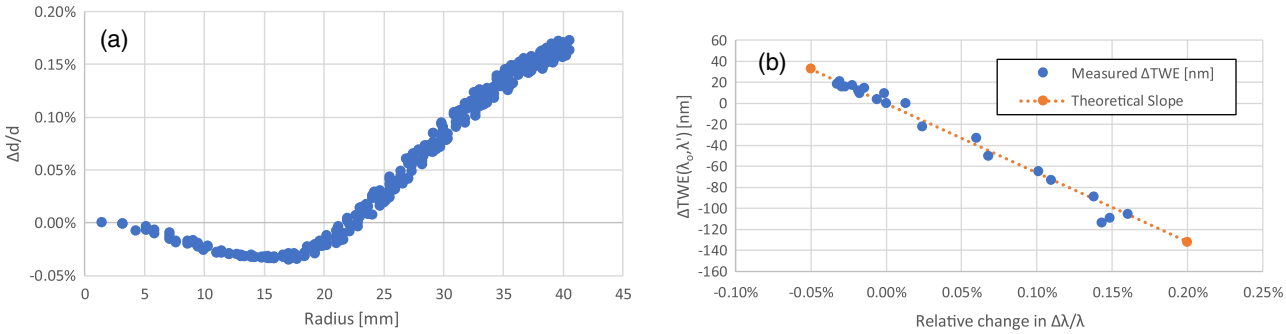


**Fig. 3.** (a) Measured thickness uniformity versus radius of the 1048 nm filter; vertical scatter is a result of an azimuthal thickness variation. (b) Measured ΔTWE based on average of two orthogonal traces of the TWE versus substrate radius of the $\lambda_o = 1048$ nm and $\lambda' = 625$ nm phase data from Fig. 2. The theoretical slope was calculated using Eq. (8) and the filter values from Table 1.

**Table 1. Theoretical Quantities of the 1048 nm Filter with $\alpha(r) = 0.19\%$**

| Wavelength (nm) | GD(λ) (ps) | $\eta(\lambda)$ | $\alpha(r) \cdot \eta(\lambda) \cdot c \cdot$ GD (nm) | $\Delta$WFD(λ) + $n_o \delta d$ (nm) |
|---|---|---|---|---|
| 625 | 0.074 | 0.961 | 40.5 | 42.8 |
| 1048 | 0.290 | 0.981 | 162.0 | 162.6 |

the approximation validity) at each radius point over the clear aperture ($r = 40$ mm) for both the in-band and out-of-band wavelengths. In Table 1, the various theoretical filter values are shown for the in-band ($\lambda_o = 1048$ nm) and out-of-band ($\lambda' = 625$ nm) wavelengths.

The values in the fourth and fifth columns show the "GD approximation" and the "exact calculation" ($\Delta$WFD, based on phase), respectively. Based on these results, Eq. (4) provides a good approximation to the exact Eq. (3).

Next, Eq. (9) is used to calculate $\Delta\text{TWE}(\lambda_o, \lambda', r)$ based on the measured $\text{TWE}(\lambda_o, r)$ and $\text{TWE}(\lambda', r)$ values, which, in Fig. 3(b), are plotted against the associated coating nonuniformity, $\alpha(r)$. To average out azimuthal variations, the measured TWE values used in this figure are an average of two orthogonal traces (spanning the clear aperture) of the TWE measurements shown in Fig. 2. Also shown in Fig. 3(b) is the theoretical slope curve calculated using the $\eta$ and GD values for $\lambda_o$ and $\lambda'$ in Eq. (8). As can be seen, there is excellent agreement showing that the previously described theoretical equations and associated approximations are valid.

The next step is to see how well the theory predicts the measured in-band TWE as a function of radius based on the out-of-band TWE. Figure 4 shows the measured TWE (with "piston"-dc offset removed) at $\lambda_o = 1048$ nm and $\lambda' = 625$ nm versus substrate radius (with no azimuthal averaging being performed in this case). The theoretical $\text{TWE}(\lambda_o, r)$ was calculated from the measured $\text{TWE}(\lambda, r)$ using the measured thickness non-uniformity values, $\alpha(r)$, and theoretical GD values of the 1048 nm filter in Eq. (8). Because the measured TWE values have an arbitrary TWE offset, it is necessary to apply a dc TWE offset to the theoretical $\text{TWE}(\lambda_o, r)$ values to line them up to the measured $\text{TWE}(\lambda_o, r)$ values. As shown, there is a good agreement between the predicted and measured TWE values at the in-band wavelength. The TWE[pv] values shown in the legend of Fig. 4 are based on the minimum/maximum TWE values for each of the TWE curves. This figure again illustrates that there is a substantial variation between the out-of-band TWE[pv] and the in-band TWE[pv] and that it is possible to predict the latter from the former using Eq. (8). Note that the measured TWE[pv] values in Fig. 4 are less than those obtained from Fig. 2 because only one "radial spoke" was investigated in Fig. 4.

It is also possible to investigate the TWE variation across the bandpass region of the 1048 nm filter using the in-band TWE measurements and compare them to theoretical predictions. These results should be even more accurate because the wavelength difference is small between the reference wavelength ($\lambda_o = 1048$ nm) and the other in-band wavelengths so that there is no significant dispersion. Figure 5(a)

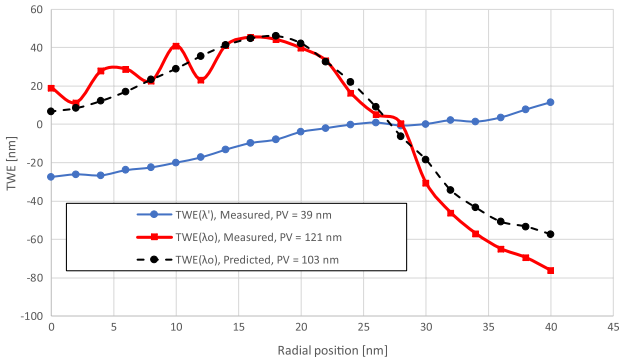


**Fig. 4.** Measured TWE (with "piston"-dc offset removed) at $\lambda_o = 1048$ nm and $\lambda' = 625$ nm versus substrate radius (and coating non-uniformity). The theoretical TWE($\lambda_o$, $r$) curve was calculated using Eq. (8), the measured TWE($\lambda'$), the measured thickness non-uniformity, $\alpha(r)$, and theoretical GD of the 1048 nm filter. The dc offset of theoretical TWE($\lambda_o$, $r$) values was adjusted to line up to the measured TWE($\lambda_o$, $r$) values. The measured and theoretical TWE[pv]($\lambda$) values listed in the legend were calculated from the min/max of the TWE($\lambda$, $r$) data.

shows the theoretical transmittance (Tx), GD, and $\varphi_T$ variation of the 1048 nm filter across the bandpass region along with the measured Tx. Note the GD variation from 0.29 to 0.43 ps across the filter bandwidth. Figure 5(b) shows the measured $\Delta$TWE($\lambda_o$, $\lambda'$)[pv] for $\lambda' = 1045 - 1053$ nm and $\lambda_o = 1048$ nm along with the theoretical $\Delta$TWE($\lambda_o$, $\lambda'$)[pv] calculated using minimum and maximum phase variation across the substrate (from $r = 0 - 40$ mm) for each $\lambda'$ at an AOI $= 3.4°$ (tilt angle of the 1048 nm filter in the wavefront sensor instrument required to avoid sending the reflected wavefront back on the sensor). Figure 5(b) demonstrates that there can be a significant TWE[pv] variation in the passband of a filter that can be easily predicted (to within $\pm$10%) based on the phase/GD variation in the passband.

Note that if the uniformity variation across the clear aperture of a bandpass filter corresponds to more than 25–50% of the filter bandwidth, then it is necessary to take into account the GD variation across the filter bandwidth to accurately calculate the effect of the coating non-uniformity on the TWE. Along these lines, to minimize the coating $\Delta$WFD of a filter, it is important to ensure that the coating non-uniformity over the filter clear aperture is less than $\sim$ 25% of the filter bandwidth (because the GD of the filter increases as the wavelength goes from the center of the filter bandpass to the edges).

One can investigate the effect of a bandpass filter steepness (for a given FWHM) on the coating $\Delta$WFD. Figure 6(a) shows the theoretical transmittance of four different 1048 nm filter designs (FWHM fixed at $\sim$ 11 nm) as the number of cavities is extended from one to four. If the maximum total coating non-uniformity is limited to 0.2% (corresponding to $\sim$ 20% of the filter's FWHM), then the GD at the center of the filter bandpass region is roughly constant across the clear aperture. Figure 6(b) shows the calculated coating $\Delta$WFD for both the out-of-band ($\lambda' = 625$ nm) and the in-band wavelengths ($\lambda_o = 1048$ nm) as the number of cavities increases from one to four, corresponding to a GD change from 0.11 to 0.29 ps, respectively. As shown, the $\Delta$WFD[pv] at the out-of-band wavelength increases from $\sim$ 5 to 22 nm as the number of cavities increases as a result of the increased coating thickness (and, hence, increased GD). At the in-band wavelength, there is a substantial increase in the $\Delta$WFD[pv] from $\sim$ 60 to 140 nm as the number of cavities increases from one to four, respectively. So, for imaging applications, increasing the steepness of a bandpass filter for a given FWHM can result in a substantial increase in the TWE of the optical filter if the coating non-uniformity is not improved. In this example, to keep the same TWE for the four-cavity filter compared to the single-cavity filter, the coating non-uniformity would have to be decreased by the ratio of the GD[four cavity]/GD[single cavity] (i.e., total non-uniformity would need to decrease by a factor of 2.5 from 0.20% to 0.08%).

For a sub-nanometer FWHM bandpass filter, the filter's GD can increase quite substantially (as does the GD variation across the filter bandpass region) compared to a 10 nm FWHM bandpass filter. For a 1048 nm bandpass four-cavity filter, as the FWHM changes from 11 to 1.1 nm (factor of 10 decrease), there is a corresponding 10-fold increase in the GD from 0.29 to 2.88 ps, respectively. However, because the uniformity needs to improve by a factor of 10 to ensure that the filter's clear aperture

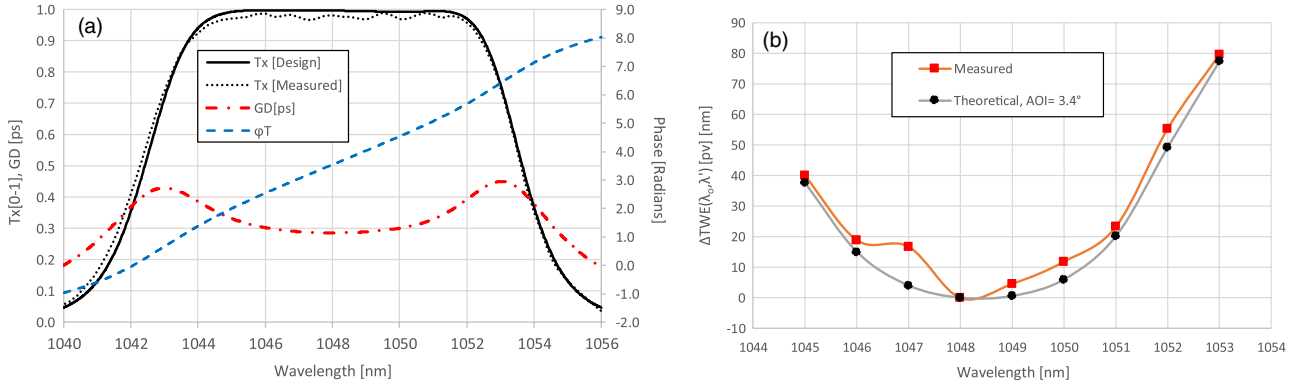


**Fig. 5.** (a) Measured Tx and theoretical Tx, GD, and $\varphi_T$ of the 1048 nm filter at normal incidence. Note the GD variation from 0.29 to 0.43 ps across the filter bandwidth. (b) Measured $\Delta$TWE($\lambda_o$, $\lambda'$)[pv] for $\lambda' = 1045 - 1053$ nm and $\lambda_o = 1048$ nm along with the theoretical $\Delta$TWE($\lambda_o$, $\lambda'$)[pv], using minimum and maximum phase variation, calculated at an AOI $= 3.4°$, across the substrate for each $\lambda'$. The AOI $= 3.4°$ was required to line up the theoretical TWE data with the measured TWE as the 1048 nm filter was tilted by this amount in the wavefront sensor instrument.

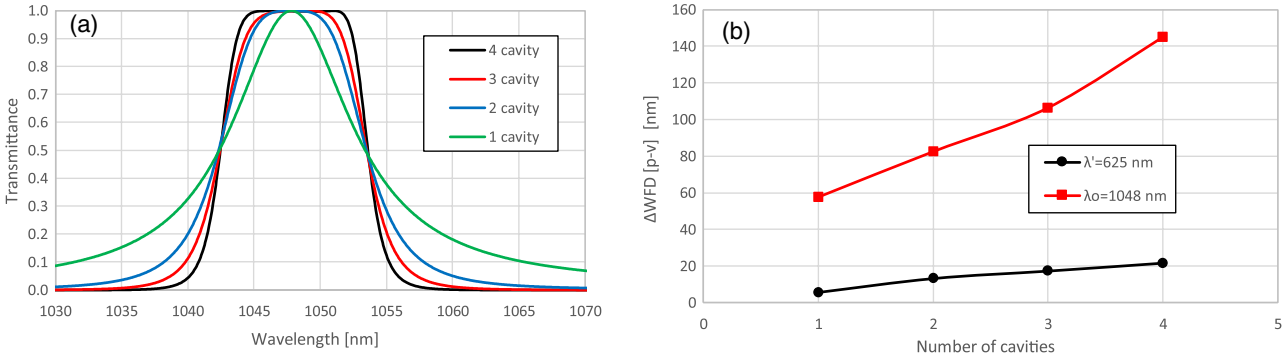


**Fig. 6.** (a) Transmittance (theory) of four designs of a 1048 nm bandpass filter with different number of cavities but the same FWHM. (b) Coating ΔWFD, based on GD approximation, versus number of cavities in the 1048 nm filter for the out-of-band wavelength ($\lambda' = 625$ nm) and the in-band wavelength ($\lambda_o = 1048$ nm).

**Table 2. Theoretical Quantities of the RWE 1052 nm Filter with $\alpha(r) = 0.46\%$**

| Wavelength (nm) | GDR(λ) (ps) | $\eta(\lambda)$ | $\alpha(r) \cdot \eta(\lambda) \cdot c \cdot$ GDR (nm) | $\Delta$RWFD(λ) + $2 \cdot n_o \delta d$ (nm) |
|---|---|---|---|---|
| 625 | 0.004 | 0.965 | 5.3 | 5.6 |
| 1052 | 0.820 | 0.980 | 1108.2 | 1120.6 |

remains the same, there is essentially no change in the coating ΔWFD[pv] other than that arising from the entrance medium contribution (because of the larger coating thickness required for the sub-nanometer bandpass while maintaining the same steepness).

## 6. RWE: DESIGN, MEASUREMENT, AND ANALYSIS

To illustrate the effect of GDR on the RWE of an optical filter, a demonstration filter with a bandpass region centered at 1052 nm was designed and grown (with an 80 mm diameter clear aperture) with the optical properties shown in Table 2.

To illustrate the effect of the RWE more clearly, the thickness non-uniformity was deliberately increased to 0.46%. As shown, the RWFD is similar for the GD approximation and the reflectance phase calculation.

The RWE of the 1052 nm demonstration filter was measured at $\lambda_o = 1052$ nm (in-band) and at $\lambda' = 625$ nm (out of-band) using the same multiwavelength wavefront sensor measurement system described previously. Figure 7(a) shows the measured RWE versus the substrate radius for the in-band and out-of-band wavelengths. Note that the RWE, unlike the TWE, is dominated by the substrate curvature, which is induced by the coating stress. As shown, there is a quite substantial difference in the RWE at the in-band and out-of-band wavelengths.

Next, the predicted in-band RWE was calculated based on the 1052 nm filter parameters and the out-of-band RWE. However, to show the accuracy of the prediction curve more clearly, the effect of the substrate curvature is removed by calculating $\Delta\text{RWE}(\lambda_o, \lambda') = \text{RWE}(\lambda_o = 1052\text{ nm}) - \text{RWE}(\lambda' = 625\text{ nm})$. The measured ΔRWE is shown in Fig. 7(b) along with the predicted ΔRWE using Eq. (11), the measured thickness non-uniformity, and the theoretical GD reflectance values. As shown, there is a reasonably good agreement (<15% difference) between the measured and predicted ΔRWE results.

The in-band RWE was also measured for this 1052 nm wavelength demonstration filter, and the predicted values were calculated. Figure 8 shows the predicted and measured $\Delta\text{RWE}(\lambda_o, \lambda')$[pv] values (as defined in the figure caption)

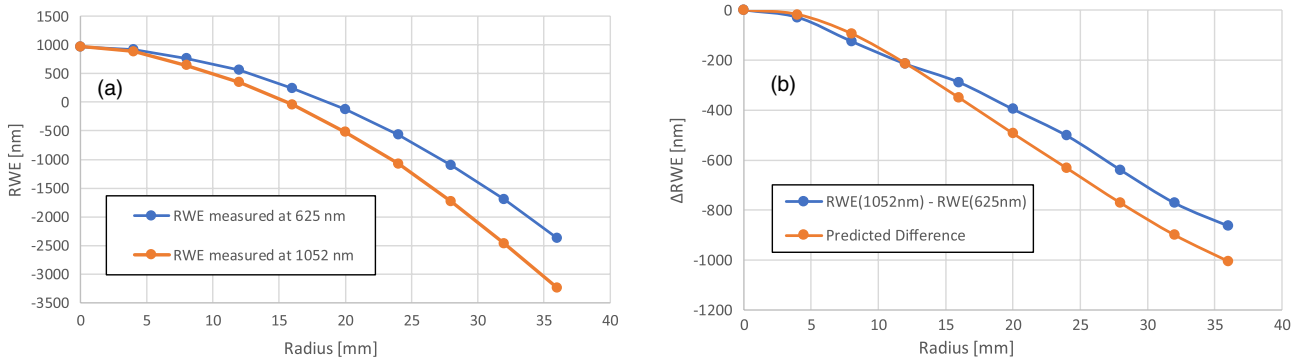


**Fig. 7.** (a) Measured RWE (with "piston"-dc offset adjusted so RWE is equal at $r = 0$ mm) at $\lambda_o = 1052$ nm and $\lambda' = 625$ nm versus substrate radius (and coating non-uniformity). Note that the RWE is dominated by the substrate curvature (coating stress induced). (b) The measured $\Delta\text{RWE}(\lambda_o, \lambda') = \text{RWE}(\lambda_o = 1052\text{ nm}) - \text{RWE}(\lambda' = 625\text{ nm})$ is shown versus substrate radius along with the predicted ΔRWE (calculated using Eq. (11), the measured RWE(λ′), the measured thickness non-uniformity, $\alpha(r)$, and theoretical GDR of the 1052 nm filter).

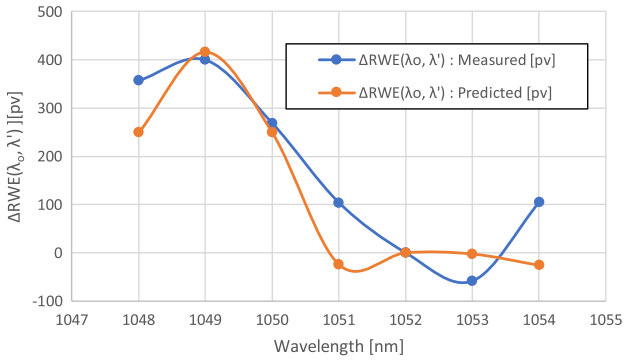


**Fig. 8.** The in-band variation in RWE[pv], normalized to the $\lambda_o = 1052$ nm wavelength, is given by $\Delta\text{RWE}(\lambda_o, \lambda') = \text{RWE}(\lambda_o = 1052\text{ nm}) - \text{RWE}(\lambda')$. In this chart, the measured and predicted $\Delta\text{RWE}(\lambda_o, \lambda')$ is shown versus the in-band wavelength.

across the filter's in-band wavelengths. Note by normalizing to center wavelength of 1052 nm, the effect of the substrate curvature is automatically removed (i.e., the RWE variation should only depend on the GDR/phase variation with wavelength). Although the overall trend is in reasonably good agreement, there are some significant differences between the predicted and measured RWE values that will require further investigation to rule out possible RWE measurement artifacts.

## 7. SUMMARY

It has been demonstrated, using measurements and theory, that the in-band TWE can be significantly different compared to an out-of-band TWE measurement, and that this difference is dependent on the coating non-uniformity and the phase properties of the optical coating. As a result, many coated surfaces measured at a nominal 633 nm interferometer wavelength may significantly underestimate the actual TWE values at the operational wavelength in which the filter is being used. This is especially true of steep narrowband filters (<1 nm bandwidth) where the GD can be very high (>5 ps). As has been verified in this paper, a theoretical prediction (using exact phase calculations or approximate GD calculations) of the in-band TWE can provide a reasonable estimate (within ±10%) of the actual in-band TWE if it cannot be measured directly. In addition, there can be a substantial variation of the TWE across a passband filter that can be predicted based on the change in GD/phase as well.

The impact on TWE as a result of increasing the steepness or modifying the bandwidth of a bandpass filter was also investigated. In practice, narrowing the bandwidth does not affect the TWE of an optical filter because the uniformity has to be improved proportionally as the GD increases. Increasing the steepness of a bandpass filter does, however, increase the TWE, but this can be compensated through reducing the thickness non-uniformity.

The extension of the TWE equations for RWE was also briefly outlined, and, similar to the TWE investigation, an RWE demonstration filter was designed, grown, measured, and analyzed. The RWE measurements at an "in-band" and "out-of-band" wavelength demonstrated that the theoretical "in-band" prediction approach works for the RWE as well. Note that although the above formulation was directly applied to bandpass filters, it can also be easily applied to any type of multilayer coating (i.e., wideband dielectric mirrors) where the TWE or RWE is of interest.

In summary, a method of determining the in-band TWE (RWE) from out-of-band TWE (RWE) measurements and the coating non-uniformity and coating phase properties has been demonstrated and verified with measurements. As well, a simple rule of thumb was derived that shows the TWE (RWE) difference between different wavelengths is proportional to the GD difference between the different wavelengths.

## APPENDIX A: DERIVATION OF GROUP DELAY WAVEFRONT DISTORTION APPROXIMATION

Restating Eq. (3),

$$\Delta\text{WFD} = \frac{-\lambda}{2\pi}\{[\varphi_T(\lambda, d+\delta d) - \varphi_T(\lambda, d)] + \varphi_o(\lambda, -\delta d)\}, \tag{A1}$$

one can expand $\varphi_T(\lambda, d+\delta d)$ using a Taylor's expansion formula:

$$\varphi_T(\lambda, d+\delta d) \approx \varphi_T(\lambda, d) + \left.\frac{\partial \varphi_T(\lambda, d)}{\partial d}\right|_d (\delta d) + \frac{1}{2}\left.\frac{\partial^2 \varphi_T(\lambda, d)}{\partial^2 d}\right|_d (\delta d)^2 + \cdots \tag{A2}$$

To first order, Eq. (A1) becomes

$$\Delta\text{WFD} \approx \frac{-\lambda}{2\pi}\left\{\left.\frac{\partial \varphi_T(\lambda, d)}{\partial d}\right|_d (\delta d) + \varphi_o(\lambda, -\delta d)\right\}. \tag{A3}$$

Now,

$$\frac{\partial \varphi_T}{\partial d} = \frac{\partial \varphi_T}{\partial \lambda}\cdot\frac{\partial \lambda}{\partial d} = \frac{\partial \varphi_T}{\partial \omega}\cdot\frac{\partial \omega}{\partial \lambda}\cdot\left(\frac{\partial \lambda}{\partial d}\right) \approx \frac{\partial \varphi_T}{\partial \omega}\cdot\frac{\partial \omega}{\partial \lambda}\cdot\left(\frac{\delta \lambda}{\delta d}\right), \tag{A4}$$

where $\omega = 2\pi c/\lambda$. If $\eta(\lambda) \equiv |(\lambda/\delta\lambda)/(d/\delta d)|$ is a function that takes into account the material optical dispersion of a coating design (and where $\eta$ can be calculated numerically from the coating design), then, rewriting this as $(\frac{\delta\lambda}{\delta d}) = \eta \cdot (\frac{\lambda}{d})$ it can be seen that

$$\frac{\partial \varphi_T}{\partial d} \approx \frac{\partial \varphi_T}{\partial \omega}\cdot\frac{\partial \omega}{\partial \lambda}\cdot\eta\cdot\left(\frac{\lambda}{d}\right) = (-\text{GD})\cdot\left(\frac{-2\pi c}{\lambda^2}\right)\cdot\eta\cdot\left(\frac{\lambda}{d}\right) = \left(\frac{2\pi}{\lambda}\right)\cdot\eta\cdot\left(\frac{1}{d}\right)\cdot\text{GD}\cdot c, \tag{A5}$$

where $\text{GD} \equiv -\frac{\partial \varphi_T}{\partial \omega}$. Then Eq. (A3) becomes

$$\Delta \mathrm{WFD} \approx \frac{-\lambda}{2\pi}\left\{\left(\frac{2\pi}{\lambda}\right)\cdot\eta\cdot\left(\frac{\delta d}{d}\right)\cdot \mathrm{GD}\cdot c+\varphi_o(\lambda,-\delta d)\right\}. \tag{A6}$$

Defining $\alpha \equiv -\delta d/d$ as the uniformity variation measured with respect to the substrate plane, and with the definition of $\varphi_o(\lambda, z)$ from Eq. (1), Eq. (A6) then becomes

$$\Delta \mathrm{WFD} \approx \alpha\cdot\{\eta\cdot \mathrm{GD}\cdot c - n_o\cdot d\cos(\theta_o)\}, \tag{A7}$$

thus deriving Eq. (4).

**Acknowledgment.** The authors would like to thank Adam Badeen for the design of the 1048 nm filter and Rebecca Saaltink for the design of the 1052 nm filter.

**Disclosures.** The authors declare no conflicts of interest.

## REFERENCES

1. J. C. Wyant and K. Creath, "Basic wavefront aberration theory for optical metrology," in *Applied Optics and Optical Engineering* (Academic, 1992), Chap. 1, Vol. **11**, pp. 1–52.
2. P. Giacomo, "Propriétés chromatiques des couches réfléchissantes multi-diélectriques," J. Phys. Radium. **19**, 307–310 (1958).
3. P. E. Ciddor, "Minimization of the apparent curvature of multilayer reflecting surfaces," Appl. Opt. **7**, 2328–2329 (1968).
4. C. K. Carniglia, "Accounting for the phase of an optical coating in an optical system," in *Frontiers in Optics* (Optical Society of America, 1999), paper WT2.
5. H. Piombini, "Estimation of phase shifts linked only to the coating for a dielectric mirror," Appl. Opt. **50**, C441–C448 (2011).
6. A. V. Tikhonravov, P. W. Baumeister, and K. V. Popov, "Phase properties of multilayers," Appl. Opt. **36**, 4382–4392 (1997).
7. P. Kupinski and H. A. Macleod, "Advances in optical manufacturing: measurement considerations when specifying optical coatings," Laser Focus World **51**, 31–38 (2015).
8. H. A. Macleod, "Phase matters," SPIE OE Mag., 29–31 (2005).
9. A. Piegari and A. Sytchkova, "Phase distortion and thickness variation in the design of optical coatings," Proc. SPIE **10562**, 1H1-4 (2016).
10. D. Fisher, "Wavefront aberrations due to optical coatings," in *Optical Interference Coatings Conference* (Optical Society of America, 2001), paper TuA6-1.
11. A. Piegari, A. Sytchkova, and M. Taccola, "Wavefront control in the design of narrow- and broad-band optical coatings," Proc. SPIE **11180**, 111804J1 (2018).
12. M. A. Quijada, L. Seide, B. A. Pasquale, J. C. McMann, J. G. Hagopian, M. Z. Dominguez, Q. Gong, and C. T. Marx, "Spectral and wavefront error performance of WFIRST/AFTA bandpass filter coating prototypes," in *2016 IEEE Aerospace Conference* (IEEE, 2016), pp. 1–13.
13. M. Vergöhl, C. Britze, S. Bruns, J. Ahrens, B. Schaefer, K. Mann, and V. Kirschner, "Development of a broadband dielectric beam splitter with reduced spectral wavefront error," Proc. SPIE **10691**, 1069118 (2018).
14. W. Boucher, Y. Priol, E. Homassel, and B. Wattellier, "Multi-wavelength large optics wave front error metrology bench," in *Optical Fabrication and Testing* (Optical Society of America, 2017), paper OM2B.2.

161.216.164.49 (as "2020-01-08 20:12:13")